CHEMICAL ENGINEERING TRANSACTIONS
VOL. 86, 2021
A publication of AIDIC
The Italian Association of Chemical Engineering
Online at www.cetjournal.it
Guest Editors: Sauro Pierucci, Jiří Jaromír Klemeš

ISBN 978-88-95608-84-6; **ISSN** 2283-9216

Design of Ventilation System to Prevent Epoxy Fume Release from Vacuum Pressure Impregnation

Yup Yoo[a,c], Jungyu Jang[a,b], Hyundo Park[a,c], Il Moon[c], Donghyun Kim[d], Baekgyu Lim[e], Hyungtae Cho[a*], Junghwan Kim[a*]

[a]Green Materials and Processes R&D Group, Korea Institute of Industrial Technology, 55, Jong-ga Road, Ulsan 44413, Republic of Korea
[b]Chemical and Biochemical Engineering, Dongguk University, 30, Pildong-ro 1-gil, Jung-gu, Seoul 04620, Republic of Korea
[c]Chemical and Biomolecular Engineering, Yonsei University, 50, Yonsei - Road, Seoul 03722, Republic of Korea
[d]Advanced Forming Process R&D Group, Korea Institute of Industrial Technology, 40, Techno - Industrial Road, Ulsan 44776, Republic of Korea
[e]MVEC Co., Ltd, 362-11, Jong-ga Road, Ulsan, 44428, Republic of Korea
htcho@kitech.re.kr; kjh31@kitech.re.kr

In this study, a model for the exhaust of epoxy fumes generated by vacuum pressure impregnation (VPI) was developed using computational fluid dynamics (CFD), and an optimal design for minimizing the fume exhaust time was developed to improve the safety of the working environment. VPI is a process of durability reinforcement by impregnating epoxy varnish insulators to the windings in the stator. In addition, the VPI process can be used for applications such as coating, sealing, and insulating porous parts. The VPI process tanks are composed of a working tank with an inner tank. As the working tank is opened after the vacuum and pressurization to proceed with the final step of the process, the epoxy fumes derived from the resin can leak into the environment. To address these safety and environmental problems, an epoxy fume exhaust process is required. Therefore, a case study was conducted using CFD to validate the exhaust efficiency of epoxy fumes by rearranging different exhaust methods. It was found that the method of using pressurization yielded a higher fume exhaust efficiency (99.46 %) than did the depressurization method (96.42 %).

1. Introduction

The vacuum pressure impregnation (VPI) process has been developed and used since the 1960s to prevent the electrical breakdown of the stator winding in generators or motors. The stator and rotor are components of a large motor or generator. In particular, the stator winding is the main component where electrical breakdown due to physical and electrical friction occurs (Kong et al., 2017). To prevent this, the resin (varnish) is mainly impregnated on it to improve the durability of the winding. In this regard, insulator resins are of a variety of different types, mainly polyester and epoxy resins. Vacuum pressurization is utilized to uniformly impregnate the epoxy resin within the impregnation tank. Most VPI processes are completed after curing the impregnated stator with epoxy resin (Bezděk, 2020). Because the curing process does not proceed inside the impregnated tank, it is necessary to open the tank and place it inside the oven. For this task, when the tank is opened, the fumes derived from the epoxy resin can leak into the working environment. To reduce the possibility of dangerous work environments, a hazardous gas exhaust system is required that utilizes an existing vent placed on the tank. However, when using the epoxy fume exhaust process, the process time is delayed owing to the curing process, and a longer process time leads to problems in insulation quality. Therefore, in this work, we minimized the process time so that the stator quality does not degrade and used existing vents to determine the optimal emission model of hazardous gases.

Usually, the probability of explosion of a flammable fume is reduced by exhausting the fume using the air inflow method. To reduce the probability of explosion hazards, monitoring the concentration of residual fumes is important (Lee et al., 2017). The most commonly used method to predict the concentration of remaining fume gases is to utilize computational fluid dynamics (CFD) (Cho et al., 2013). Lambaert et al. (2010) developed an effective tool for ventilation validation studies although the simulation results showed an error ratio of 5.2 % with respect to the experimental ones. Within large tendencies, this is an acceptable range for fume flow prediction. In this study, CFD is utilized for predicting the epoxy fume concentration according to the air flow inside the tank and determining the optimal condition among several cases (Dahal et al., 2016).
This study aims to identify the flow of fumes derived from epoxy resin using CFD, compare the depressurization compression method using three vents, and determine the optimal conditions. Section 2 presents the procedure of the commercial VPI process and the CFD simulation conditions utilized. Section 3 focuses on the causal analysis of the CFD results and the efficiency of fume exhaust for each set of cases. Finally, Section 4 concludes the paper, summarizing the optimal fume exhaust case and further research to be conducted.

2. Methodology

2.1 VPI commercial process

The entire VPI process is illustrated in Figure 1. In stage 1, a vacuum is formed using a vacuum pump to suppress air bubbles. In stage 2, the epoxy resin is injected. The next step involves extracting the epoxy resin after impregnating the stator with insulation through pressurization, decompression and shipping the stator after curing in the oven. During this stage, large amounts of epoxy resin-derived fumes fill the tank. In stage 4, the fumes generated from the epoxy resin leak into the working environment. To improve the environment for workers, the overall process stability needs to be increased by adding an exhaust process for the hazardous gases in the existing stage 4. Additionally, it is necessary to minimize the delay time of the curing stage so that the quality of the stator insulation does not deteriorate.
The VPI tank consists mainly of a working tank (5200 H × 4500 ⌀, mm) and an inner tank (3100 W × 3100 L × 3410 H, mm) (Figure 2). The vessel that injects epoxy resin and directly impregnates the stator is the inner tank. The VPI tank utilizes a total of three existing vents, A (250 ⌀), B (80 ⌀), and C (100 ⌀), to avoid additional costs. A pump that moves fumes with a dust collector has the capacity to form a pressure of 250 mmAq.

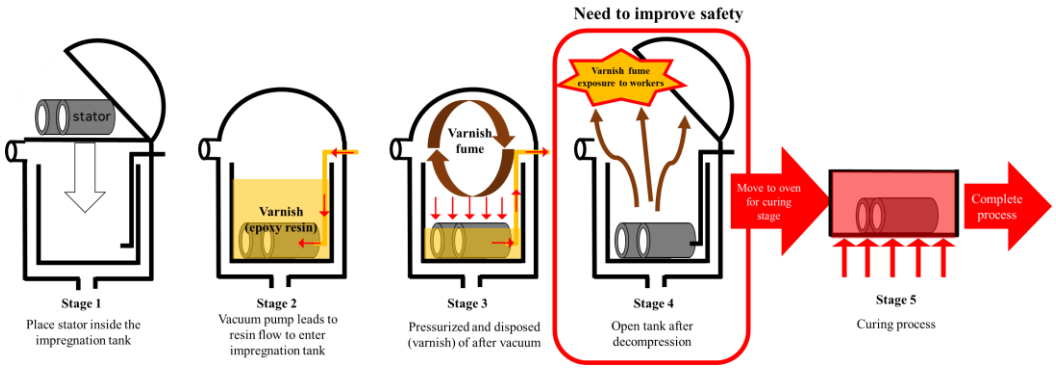

Figure 1: Schematic diagram of the VPI process

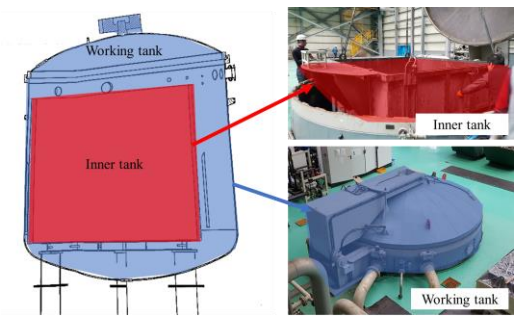

Figure 2: VPI tank configuration overview

2.2 CFD Simulation

2.2.1 Geometry

The CFD model geometry was developed in cooperation with SpaceClaim. Figure 3 depicts the CFD model geometry with the actual location of each vent, A (250 ⌀), B (80 ⌀), and C (100 ⌀), in the overall geometry. The working tank (5200 H × 4500 ⌀, mm) and inner tank (3100 W × 3100 L × 3410 H, mm) were designed to create a structure with one stator in the inner tank.

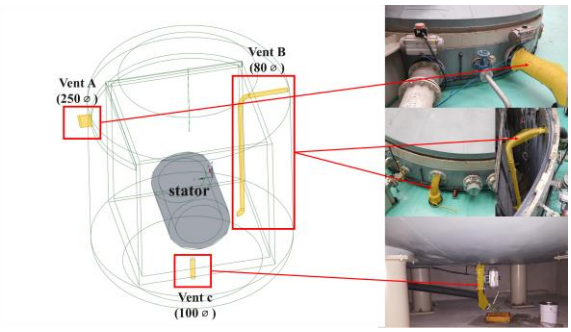

Figure 3: Geometry of VPI tank for CFD

2.2.2 Mesh

The geometry was created using a quadratic-type mesh. A high mesh density was used for areas around A, B, and C, where the gas flow is fast or a relatively high pressure exists, to increase the accuracy of the analytical results. Approximately 15 million elements with 22 million nodes were generated by using the proximity and curvature mesh size functions (Figure 4).

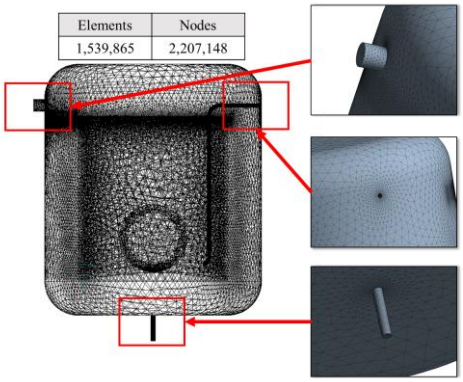

Figure 4: Mesh configuration of the geometry

2.2.3 Boundary condition and solver

The commercially available CFD software ANSYS Fluent 19.0 was used in this study to predict the fume exhaust efficiency in the working tank. The Eulerian multiphase model was used because a single pressure is shared by all phases, and the momentum and continuity equations were solved for each. The multiphase turbulence model per phase was used to identify turbulent flow in each phase, and the realizable K-epsilon model was used to solve such turbulent flow conditions. It was assumed that the fumes filled the tank in stage 4 of the VPI process. The scenario of the exhaust method through air inflow and the exhaustion of fumes from one vent was analyzed. Using the transient method, a time step of 0.05 s was set, analysis was conducted using a total run time of 1200 s, and gravity was defined by 9.8 m/s^2. The results were interpreted by extracting data every 200 s. The total area of the flow field was approximately 73 m^3. The volume fraction of the fumes was observed in the total flow field, and the amount of residual fumes was monitored. Using vents A, B, and C, a total of six boundary conditions of the cases considered are shown in Table 1.

Table 1: Boundary conditions for different cases

	Case 1	Case 2	Case 3	Case 4	Case 5	Case 6
Inlet (pressure)	Vents B, C (Operating pressure)	Vents A, C (Operating pressure)	Vents A, B (Operating pressure)	Vent A (2452 Pa)	Vent B (2452 Pa)	Vent C (2452 Pa)
Outlet (pressure)	Vent A (-2452 Pa)	Vent B (-2452 Pa)	Vent C (-2452 Pa)	Vents B, C (Operating pressure)	Vents A, C (Operating pressure)	Vents A, B (Operating pressure)

3. Results

Figure 5 shows the plot of the fume exhaust efficiency, determined using Eq. (1) below, for the three cases.

$$\frac{Exhausted\ fume\ volume}{Initial\ fume\ volume} \times 100 = Fume\ exhaust\ efficiency\ (\%) \quad (1)$$

After 1200 s, the depressurization method showed the highest efficiency for case 1 (exhausted to Vent A) at 96.42 %. The highest fume exhaust efficiency was measured at 99.46 % when introduced into vent A during the inflow method. On the contrary, cases 2 and 3, and cases 5 and 6 using vents B and C, respectively, exhibited relatively low fume exhaust efficiencies. In particular, a fume exhaust efficiency of 98.3 % was seen for case 4 at 923 s, while the remaining fumes were reduced to less than 1.7 vol %. This volume is set based on the lower explosive limit (LEL) of the epoxy resin.

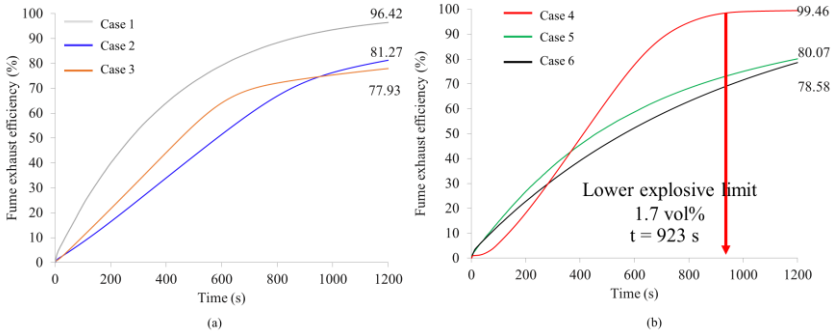

Figure 5: Comparison of fume exhaust efficiency according to different cases in (a) depressurization method, and (b) pressurization method

Figure 6 shows the fume volume fraction according to time in the inhalation method for cases 2 and 3. In case 2, the fumes that filled the inner tank were first discharged due to depressurization from vent B. Simultaneously, air was inhaled from vent A due to the negative pressure formation. At vent C, a pressure greater than the pressure of fumes must be formed at the boundary to allow the entry of air. A problem of backflow was observed, indicating that the negative pressure formed at vent A did not reach vent C. The same problem occurred in case 3. It is believed that such conditions for cases 2 and 3 may also cause tank safety problems due to the backflow problem.

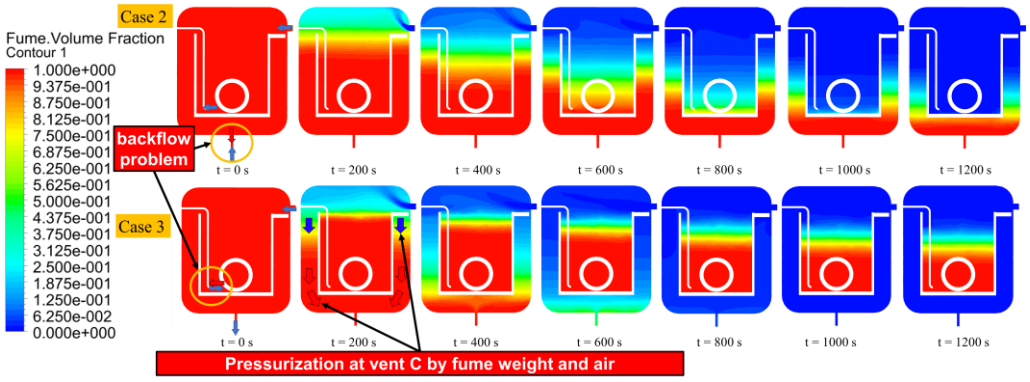

Figure 6: Changes in the fume contour for cases 2 and 3 according to time

Figure 7 shows the fume exhaust in cases 5 and 6 of pressurization over time. The pressurization method showed no backflow problem, as seen in cases 2 and 3, so the fume was released stably. The fume had a higher density than that of air and flowed under the tank. Thus, as identified in case 5, the effect of fume pressure resulted in a large ΔP of vent C (outlet), leading to a rapid fume exhaustion. For pressurization, it is considered most appropriate if the outlet is located under the tank.

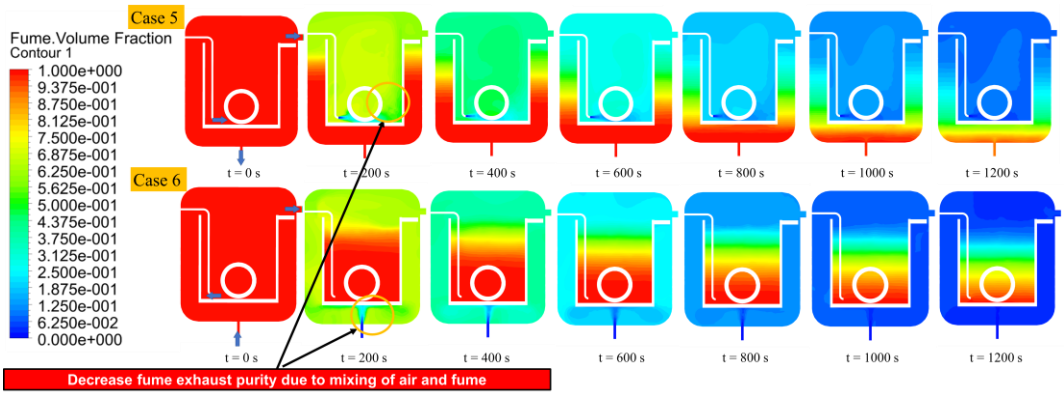

Figure 7: Changes in the fume contour for cases 5 and 6 according to time

Figure 8 shows a comparison between case 4 having the highest exhaust efficiency in the pressurization method and case 1 having the same in the depressurization method. The negative pressure did not reach the other air inlet vent under depressurization conditions in cases 2 and 3. However, pressure drops of -1508.58 to -1587.06 Pa for vent B and -1177.2 to -1587.06 Pa for vent C were seen. Thus, in case 1, air inflow rates of 49.58–57.44 m/s at vent B and 42.84–50.90 m/s at vent C were observed as seen in Figure 9(a). The pressure drop at vent C was weaker than that at vent B because of the pressure that the fumes created. In case 4, air flow rates of 5.09–11.3 m/s were observed at vent C. Case 4 showed the highest exhaust efficiency despite the low exhaust flow rate because of the high purity of the continuous fumes. In case 1, the air flow rate was high, and air and fumes were mixed from the beginning, making it impossible to exhaust high-purity fumes continuously. In case 4, however, vent A showed exhaust fumes with minimal mixing of air and fumes at a relatively low air flow rate (Figure 9(b)). Therefore, case 4 was determined to be the most efficient fume exhaust condition. The epoxy resin used in this study was a CAS number 3409-76-1 substance whose main constituent is methyl-tetrahydromethylphthalic anhydride. The flammability range of this material is 1.7–10.5 %, which suggests that the ideal exhaust time for case 4 is approximately 923 s based on the LEL.

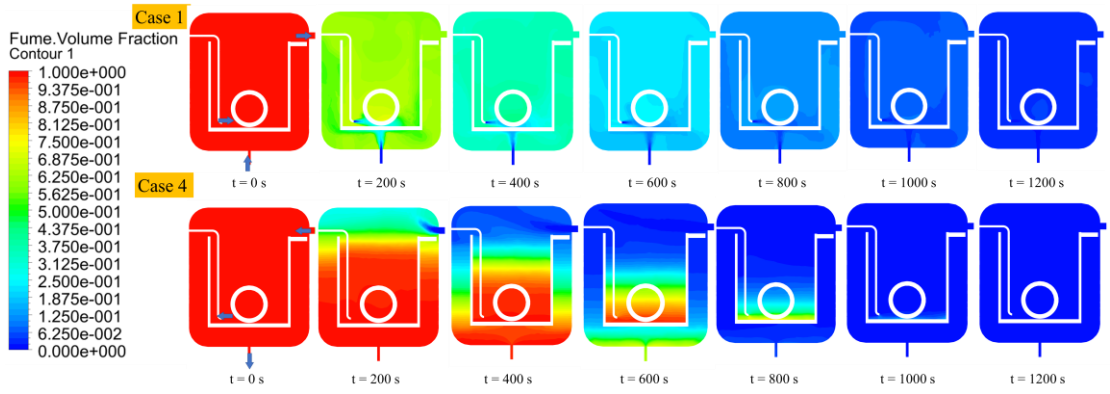

Figure 8: Changes in the fume contour of cases 1 and 4 according to time

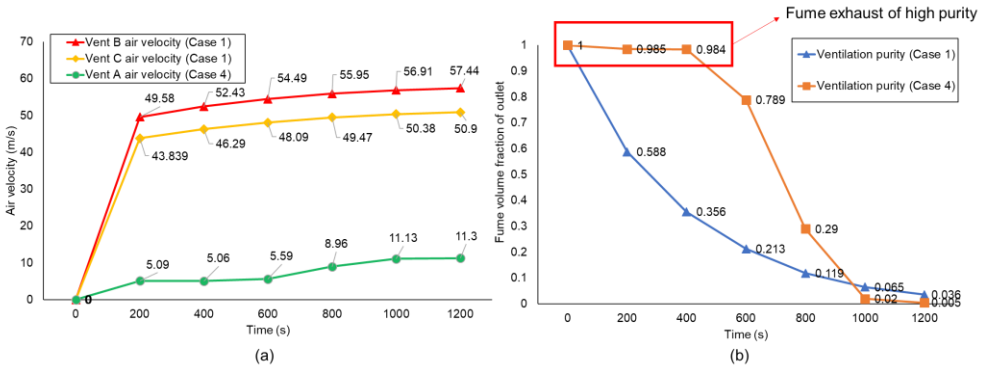

Figure 9: (a) Air inlet flow rate monitoring, and (b) Fume exhaust purity of cases 1 and 4

4. Conclusions

In this study, an optimal model for the exhaust of epoxy fumes generated from the VPI process was determined by classifying the depressurization and pressurization methods, and the fume concentration was predicted using CFD for a total of six cases. Based on the LEL, we selected a case that exhausted epoxy fume with a minimal time of up to a low explosion risk concentration. The highest fume-exhaust efficiencies for the depressurization and pressurization methods were observed the transient analysis method. Vent C in case 2 and vent B in case 3 were not able to allow the air to enter due to pressure created by the fumes. Backflow problems occurred in these cases. However, the pressure created by the fumes to ensure its fast exhaust was utilized in cases 5 and 6. The fumes were mixed with air in the tank due to high air inlet flow rate. This prevented the exhaust of high-purity fumes, and a low fume exhaust efficiency was observed. Case 1 had a fume exhaust efficiency of 96.42 %, but it was lower than that of case 4 because of a mixture of incoming air and fumes. A slow air flow rate prevented air mixing, it led to the release of high-purity fumes. The fume exhaust efficiency was the highest in case 4. Thus, case 4, which can reach the LEL, was determined to be the most appropriate condition, and the appropriate fume exhaust time was derived to be 923 s. The flow pattern may change significantly depending on the concentration of fumes. Therefore, further research is needed to determine the appropriate fume emission time range according to the concentration of fumes.

Acknowledgments

This study has been conducted with the Korea Institute of Industrial Technology as "Development of AI Platform Technology for Smart Chemical Process (JH-20-0005)".

References

Bezděk, Z., 2020, New VPI Insulation System of High Voltage Stator Windings of Large Rotating Electrical Machines Based on Cogemica VPI Tapes and One-component Epoxy Impregnation Varnish, International Conference on Diagnostics in Electrical Engineering, 1-5, http://10.1109/Diagnostika49114.2020.9214660

Cho, H., Cha, B., Kim, S., Ryu, J., Kim, J., Moon, I., 2013, Numerical analysis for particle deposit formation in reactor cyclone of residue fluidized catalytic cracking, Industrial & Engineering Chemistry Research, 52(22), 7252-7258, https://doi.org/10.1021/ie302509q

Dahal, S., Kim, T., Ahn, K., 2016, Indirect prediction of welding fume diffusion inside a room using computational fluid dynamics, Atmosphere, 7(6), 74, https://doi.org/10.3390/atmos7060074

Kong, T., Kim, H., Lee, S., & Park, J., 2017, A Study on Insulation Properties of Global VPI Type Generator through Replacement of Stator Windings, KEPCO Journal on Electric Power and Energy, 3(2), 113–117. https://doi.org/10.18770/KEPCO.2017.03.02.113

Lambert, A. R., Lin, C. L., Mardorf, E., O'shaughnessy, P., 2010, CFD Simulation of contaminant decay for high reynolds flow in a controlled environment, Annals of occupational hygiene, 54(1), 88-99, https://doi.org/10.1093/annhyg/mep057

Lee, J., Cho, S., Park, C., Cho, H., Moon, I., 2017, Numerical analysis of hydrogen ventilation in a confined facility with various opening sizes, positions and leak quantities, In Computer Aided Chemical Engineering, 40, 559-564, https://doi.org/10.1016/B978-0-444-63965-3.50095-7